

The role of CP violating scatterings in baryogenesis — case study of the neutron portal

Iason Baldes,^a Nicole F. Bell,^a Alexander Millar,^a Kalliopi Petraki^b and Raymond R. Volkas.^a

^aARC Centre of Excellence for Particle Physics at the Terascale, School of Physics, The University of Melbourne, Victoria 3010, Australia

^bNikhef, Science Park 105, 1098 XG Amsterdam, The Netherlands

E-mail: i.baldes@student.unimelb.edu.au, n.bell@unimelb.edu.au, a.millar@student.unimelb.edu.au, kpetraki@nikhef.nl, raymondv@unimelb.edu.au

Abstract. Many baryogenesis scenarios invoke the charge parity (CP) violating out-of-equilibrium decay of a heavy particle in order to explain the baryon asymmetry. Such scenarios will in general also allow CP violating scatterings. We study the effect of these CP violating scatterings on the final asymmetry in a neutron portal scenario. We solve the Boltzmann equations governing the evolution of the baryon number numerically and show that the CP violating scatterings play a dominant role in a significant portion of the parameter space.

Keywords: baryon asymmetry, CP violation, scatterings

Contents

1	Introduction	1
2	Notation	2
3	Neutron portal	3
3.1	Lagrangian	3
3.2	Decays	4
3.3	Scatterings	6
4	Boltzmann equations	8
4.1	Differential equations	8
4.2	Chemical potentials	9
4.3	Numerical solutions	11
5	Constraints	14
6	UV completions	15
7	Conclusion	16
A	Unitarity constraint for multiple quark generations	17
B	Cross sections, decay rates and CP violation	18

1 Introduction

A baryon symmetric universe would result in a baryon density around ten orders of magnitude smaller than observed [1]. Deductions of the baryon asymmetry from the cosmic microwave background give a baryon-to-entropy density ratio of [2, 3],

$$Y_B = (0.86 \pm 0.01) \times 10^{-10}, \quad (1.1)$$

which is in agreement with the baryon asymmetry required to match observed primordial element abundances: $0.4 \times 10^{-10} \lesssim Y_B \lesssim 0.9 \times 10^{-10}$ [4]. The required baryon asymmetry can be created dynamically by scenarios satisfying the Sakharov conditions [5]. One way of producing an asymmetry is through the out-of-equilibrium and CP violating decays of a heavy particle such as in leptogenesis or grand unified theory baryogenesis [6–9].

Scatterings of particles in $2 \leftrightarrow 2$ type processes can also violate CP and potentially produce asymmetries. In such scenarios, the out-of-equilibrium condition can be satisfied in two ways. The first option is to have a visible and a hidden sector at different temperatures [10–12]; the second is to have one or more of the particles freeze out, such as the annihilating DM particles in WIMPy baryogenesis scenarios [13–17]. The general principles behind such a freeze out scenario have been investigated in ref. [18]. CP violation in $2 \leftrightarrow 2$ processes could also provide a mechanism for producing asymmetric dark matter [19–22] in both freeze-in [10–12] and freeze-out type scenarios [18, 23].

The presence of CP violation in scatterings is, however, not confined to models specifically constructed to exploit this feature: it can also appear in baryogenesis-via-decay type scenarios. For example, scatterings of the heavy Majorana neutrinos in leptogenesis also violate CP [24–28]. Numerical calculations show including CP violating scatterings in leptogenesis has a large effect on the baryon asymmetry at high temperature but only a negligible effect at low temperature [24]. The purpose of this paper is to study the effects of CP violating scatterings on the generation of the baryon asymmetry more generally. We choose to study a neutron portal model in which the parameters are not restricted by having to explain low energy neutrino data. Baryogenesis via CP violating decays in the neutron portal have been studied previously [29]. CP violating scatterings in a neutron portal model were discussed in ref. [23]; however, the unitarity constraint was not properly taken into account. We will extend the analysis to include a full numerical treatment of the Boltzmann equations including CP violating scatterings. Such effects are not constrained to this particular model and will play a role in baryogenesis scenarios more generally.

The layout of the paper is as follows. In section 2 we introduce our notation. In section 3 we introduce the neutron portal Lagrangian and discuss the relevant decays and scatterings. In section 4 we write down the Boltzmann equations for the evolution of the baryon asymmetry and show example numerical solutions. Constraints on the model are discussed in section 5. Possible UV completions are discussed in section 6.

2 Notation

In an expanding universe with no collisions, a particle number density, n_X , drops as R^{-3} where R is the scale factor. Taking into account collisions the density evolves as:

$$\frac{dn_X}{dt} + 3Hn_X = C(X), \quad (2.1)$$

where $H = \dot{R}/R$ is the Hubble expansion rate and $C(X)$ is the collision term, i.e. the rate of change of n_X due to interactions with other particles. Let us imagine now such an interaction from state α to state β and its reverse process which changes X number by one unit. The collision term for this transition can be written as [30]:

$$C_{\alpha\beta}(X) = \int \dots \int d\Pi_{\alpha_1} \dots d\Pi_{\alpha_n} d\Pi_{\beta_1} \dots d\Pi_{\beta_m} \delta^4 \left(\sum p_i - \sum p_j \right) (2\pi)^4 \\ \times \left\{ f_{\beta_1} \dots f_{\beta_m} |\mathcal{M}(\beta \rightarrow \alpha)|^2 - f_{\alpha_1} \dots f_{\alpha_n} |\mathcal{M}(\alpha \rightarrow \beta)|^2 \right\}, \quad (2.2)$$

where $f_\psi = \text{Exp}[(\mu_\psi - E_\psi)/T]$ is the phase space density of species ψ with chemical potential μ_ψ at energy E_ψ and temperature T ,

$$d\Pi_\psi = \frac{g_\psi d^3 p_\psi}{2E_\psi (2\pi)^3} \quad (2.3)$$

is the normalised volume element of the three momentum and g_ψ counts the degrees of freedom of ψ . As an approximation we have used Maxwell-Boltzmann statistics and so have dropped the stimulated emission factors and Pauli blocking terms appropriate for the full quantum statistics. We assume kinetic equilibrium, i.e. a common temperature T ,

throughout. We denote the equilibrium reaction rate density for a process $\alpha \rightarrow \beta$ as:

$$W(\alpha \rightarrow \beta) \equiv \int \dots \int d\Pi_{\alpha_1} \dots d\Pi_{\alpha_n} d\Pi_{\beta_1} \dots d\Pi_{\beta_m} \delta^4 \left(\sum p_i - \sum p_j \right) (2\pi)^4 f_{\alpha_1}^{eq} \dots f_{\alpha_n}^{eq} |\mathcal{M}(\alpha \rightarrow \beta)|^2 \\ \equiv n_{\alpha_1}^{eq} \dots n_{\alpha_n}^{eq} \langle v\sigma(\alpha \rightarrow \beta) \rangle, \quad (2.4)$$

where $\langle v\sigma(\alpha \rightarrow \beta) \rangle$ is the thermally averaged cross section and $f_{\alpha_i}^{eq}$ ($n_{\alpha_i}^{eq}$) denotes the phase space (particle number) density in the absence of a chemical potential. Using Maxwell-Boltzmann statistics:

$$n_{\alpha_i}^{eq} = \frac{g_{\alpha_i} M_{\alpha_i}^2 T}{2\pi^2} K_2 \left(\frac{M_{\alpha_i}}{T} \right), \quad (2.5)$$

where M_{α_i} is the mass of the species and $K_2(x)$ is the modified Bessel function of the second kind of order two. In the Maxwell-Boltzmann approximation, the non-equilibrium rate is found using the appropriate re-weighting:

$$W^{\text{neq}}(\alpha \rightarrow \beta) = \frac{n_{\alpha_1} \dots n_{\alpha_n}}{n_{\alpha_1}^{eq} \dots n_{\alpha_n}^{eq}} W(\alpha \rightarrow \beta). \quad (2.6)$$

Unitarity of the S-matrix and invariance under charge parity time (CPT) gives a condition for the equilibrium rate densities [6, 7]:

$$\sum_{\beta} W(\alpha \rightarrow \beta) = \sum_{\beta} W(\beta \rightarrow \alpha) = \sum_{\beta} W(\bar{\beta} \rightarrow \bar{\alpha}) = \sum_{\beta} W(\bar{\alpha} \rightarrow \bar{\beta}), \quad (2.7)$$

where the sum runs over all possible final states and $\bar{\alpha}$ denotes the CP conjugate of α . This ensures no particle number asymmetry can be generated without a departure from equilibrium [31–33].

3 Neutron portal

3.1 Lagrangian

Consider the interaction Lagrangian [29],

$$\Delta\mathcal{L} = \kappa_{1ijk} \overline{X_{1L}} u_{Ri} \overline{(d_{Rj})^c} d_{Rk} + \kappa_{2ijk} \overline{X_{2L}} u_{Ri} \overline{(d_{Rj})^c} d_{Rk} + \kappa_{3ij} \overline{u_{Ri}} X_{1L} \overline{X_{2L}} u_{Rj} \\ + \frac{1}{2} \kappa_{4ij} \overline{u_{Ri}} X_{1L} \overline{X_{1L}} u_{Rj} + \frac{1}{2} \kappa_{5ij} \overline{u_{Ri}} X_{2L} \overline{X_{2L}} u_{Rj} + H.c., \quad (3.1)$$

where the κ_{aijk} are couplings with units of $(\text{mass})^{-2}$, u_{Ri} (d_{Ri}) is the right chiral up (down) type quark field of flavour i , Ψ^c denotes the conjugate of field Ψ and the X_{α} are Majorana fermions. We impose a global lepton number symmetry forbidding coupling of the X_{α} to the standard model (SM) Higgs and lepton doublets. Spinor indices are contracted between the first two and last two fermion fields in each of the terms. We have suppressed colour indices. Due to the antisymmetric colour index and the identity $\overline{\Psi}\chi^c = \bar{\chi}\Psi^c$ the couplings κ_{1ijk} and κ_{2ijk} are necessarily antisymmetric in down type quark flavour.

Other operators in addition to the ones of eq. (3.1) are allowed by the symmetries of the theory e.g. $\overline{d_{Ri}} X_{1L} \overline{X_{2L}} d_{Rj}$. For simplicity we take such operators to be sufficiently suppressed compared to those of eq. (3.1) as to be negligible. Even if present these would not qualitatively alter the outcomes below.

The decays of the heavier X_α — from now taken to be X_2 — can be CP violating and if they occur out-of-equilibrium will lead to a baryon asymmetry. However, as we will see below, scatterings of the form $u_i X_{\alpha L} \rightarrow \overline{d_j d_k}$ also violate CP: we will study the effects of this CP violation on the final asymmetry.

The above Lagrangian contains 28 physical phases if one considers couplings to all possible flavour combinations. As a demonstration and in order to simplify the analysis we will restrict ourselves to considering only couplings to the first generation up quark and second and third generation down quarks, s and b . From now on we will suppress flavour indices on the above couplings. After rephasing we are left with two physical phases. For simplicity we set:

$$\kappa_1 = e^{i\pi/2} |\kappa_1|, \quad (3.2)$$

while we set the other phase (of κ_3) to zero. This choice for the phases leads to the largest CP violation: if the final asymmetry exceeds the observed one the asymmetry can always be reduced by decreasing the κ_1 phase. The other couplings are taken to be real.

3.2 Decays

The tree level decay rate $\Gamma(X_\alpha \rightarrow usb) + \Gamma(X_\alpha \rightarrow \overline{usb})$ is:

$$\Gamma_{\alpha A} = \frac{|\kappa_\alpha|^2 (M_{X_\alpha})^5}{512\pi^3}, \quad (3.3)$$

where we have ignored the masses of the final state particles. X_2 has an additional decay channel with rate $\Gamma(X_2 \rightarrow X_1 u \bar{u})$:

$$\Gamma_{2B} = \frac{|\kappa_3|^2 (M_{X_2})^5}{1024\pi^3} \quad (3.4)$$

where we have ignored the masses of the final state particles (the full integral expression for massive X_1 can be found in appendix B).

CP violation in the decays of X_2 arises from the interference between the tree and one loop diagrams depicted in figure 1. We parameterise the CP violation in the X_2 decay in the following way:

$$\Gamma(X_2 \rightarrow usb) = \frac{1}{2}(1 + \epsilon_D)\Gamma_{2A}, \quad (3.5)$$

$$\Gamma(X_2 \rightarrow \overline{usb}) = \frac{1}{2}(1 - \epsilon_D)\Gamma_{2A}. \quad (3.6)$$

The CP violation can be calculated in terms of the underlying parameters of the theory by using the Cutkosky rules to extract the imaginary component of the interference term [34]. The results are shown in figure 2 and further details can be found in appendix B. From dimensional arguments one expects,

$$\epsilon_D \sim \frac{1}{16\pi} \frac{\text{Im}[\kappa_1^* \kappa_2 \kappa_3^*]}{|\kappa_2|^2} M_{X_2}^2 \sim \frac{\kappa}{16\pi} M_{X_2}^2, \quad (3.7)$$

in the massless limit for X_1 , where the second relation follows for couplings of a similar magnitude $\mathcal{O}(\kappa_a) \sim \kappa$ and an order one phase. This is confirmed by our detailed calculation, as can be seen in figure 2.

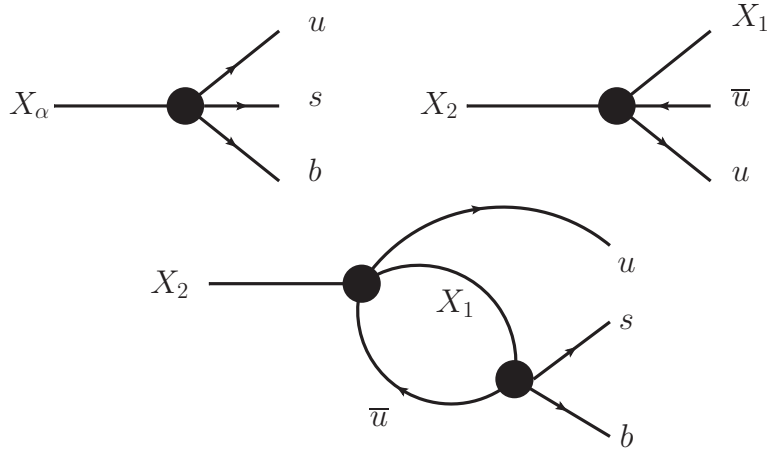


Figure 1. Tree and loop level decays for X_1 and X_2 . The particles in the loop for the lower diagram can go on-shell: interference between this and the tree diagram leads to CP violation in the X_2 decay. The X_2 in the loop in the analogous X_1 decay diagram cannot go on-shell and consequently there is no CP violation in the X_1 decay.

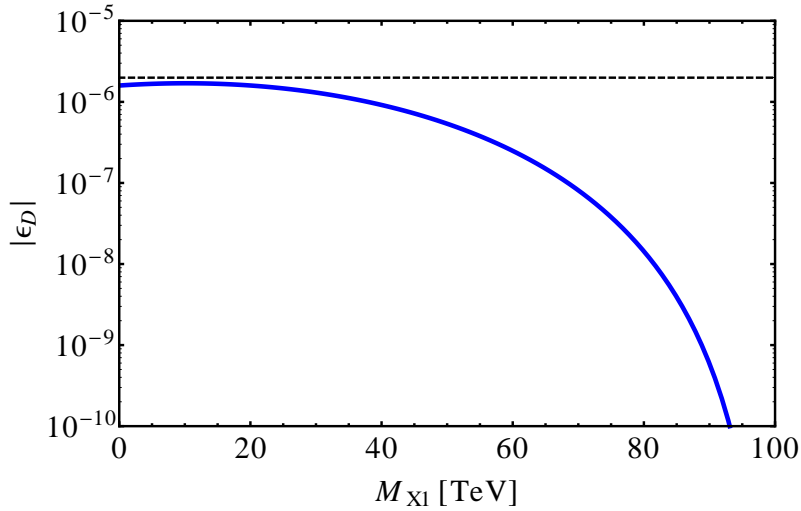


Figure 2. CP violation in the decay of X_2 with $M_{X_2} = 100$ TeV and $\kappa_a = 10^{-14}$ GeV $^{-2}$ as a function of M_{X_1} . The horizontal dashed line corresponds to $\epsilon_D = \frac{\kappa_a}{16\pi} M_{X_2}^2$.

One must also take into account CP violation in the scattering process $usb \rightarrow \overline{usb}$ mediated by an X_2 with the real intermediate part of the scattering subtracted [7]. We define this rate as:

$$W(usb \rightarrow \overline{usb}) = (1 + \epsilon_{OS})W_{OS} \quad (3.8)$$

where the CP conjugate can be found by taking $\epsilon_{OS} \rightarrow -\epsilon_{OS}$. The unitary condition (2.7) — taking usb as the initial state and summing over all possible final states — enforces the relation:

$$\epsilon_{OS}W_{OS} = \frac{1}{2}\epsilon_D n_2^{eq} \Gamma_{2A}. \quad (3.9)$$

This CP violating rate balances the CP violation in the decays when X_2 is in thermal equilibrium [7] and is included in our Boltzmann equations below. The CP symmetric washout rates $W(usb \rightarrow \overline{usb})$, mediated by off shell X_1 and X_2 , are $\mathcal{O}(\kappa^4)$ and are negligible for the parameters we are interested in below: these have been omitted from the Boltzmann equations.

3.3 Scatterings

Next we turn our attention to the scatterings. CP violation arises due to the interference between the tree and one-loop diagrams such as those depicted in figure 3. We parameterise the relevant CP violating equilibrium collision terms as:

$$W(u + X_1 \rightarrow \bar{s} + \bar{b}) = (1 + \epsilon_1)W_1, \quad (3.10)$$

$$W(u + X_2 \rightarrow \bar{s} + \bar{b}) = (1 + \epsilon_2)W_2, \quad (3.11)$$

$$W(u + X_1 \rightarrow u + X_2) = (1 + \epsilon_3)W_3, \quad (3.12)$$

where the CP conjugate interaction rate can be found by making the substitution $\epsilon_i \rightarrow -\epsilon_i$. These interactions will contribute to the baryon asymmetry. The unitarity conditions for these interactions give:¹

$$\epsilon_1 W_1 + \epsilon_2 W_2 = 0, \quad (3.13)$$

$$\epsilon_1 W_1 + \epsilon_3 W_3 = 0, \quad (3.14)$$

$$\epsilon_2 W_2 - \epsilon_3 W_3 = 0. \quad (3.15)$$

CP conserving (to the order we are working) collision terms are also present; we denote them in the following way:

$$W(s + X_1 \rightarrow \bar{u} + \bar{b}) = W_4, \quad (3.16)$$

$$W(s + X_2 \rightarrow \bar{u} + \bar{b}) = W_5, \quad (3.17)$$

$$W(X_1 + X_1 \rightarrow u + \bar{u}) = W_6, \quad (3.18)$$

$$W(X_2 + X_2 \rightarrow u + \bar{u}) = W_7, \quad (3.19)$$

$$W(X_1 + X_2 \rightarrow u + \bar{u}) = W_8. \quad (3.20)$$

We calculate the relevant cross sections and find the thermal averaged cross sections numerically by making use of the single integral formula [35]:

$$\langle v\sigma(ij \rightarrow kl) \rangle = \frac{g_i g_j T}{8\pi^4 n_i^{eq} n_j^{eq}} \int_{(m_i+m_j)^2}^{\Lambda^2} p_{ij} E_i E_j v \sigma K_1 \left(\frac{\sqrt{\hat{s}}}{T} \right) d\hat{s}, \quad (3.21)$$

where \hat{s} is the centre-of-mass energy squared, p_{ij} is the initial centre-of-mass momentum, $K_1(x)$ is the modified Bessel function of the second kind of order one and Λ is the effective theory cut-off. The expressions for the cross sections can be found in appendix B.

The CP violation in the scatterings at the cross section level i.e. the difference between the cross section and its CP conjugate, $(\sigma - \bar{\sigma})$, can be calculated in terms of the underlying

¹The unitarity condition for couplings to all possible quark flavour combinations is discussed in appendix A.

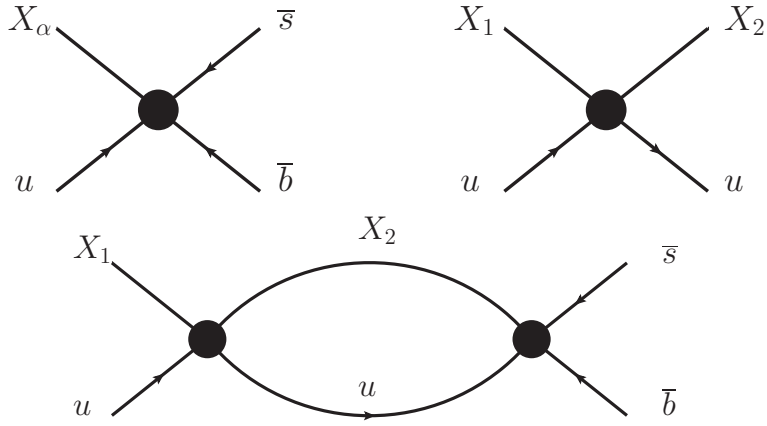


Figure 3. Example tree and loop level scatterings leading to CP violation. Further loop diagrams exist with e.g. X_1 and X_2 interchanged.

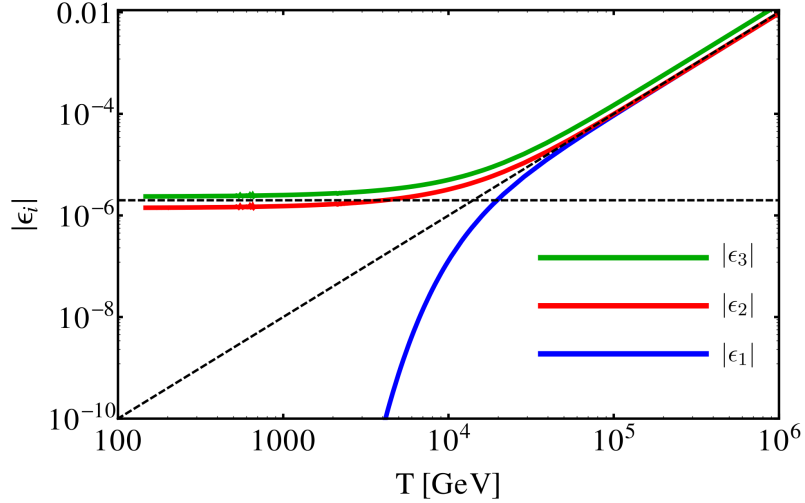


Figure 4. CP violation in the scatterings with $M_{X_2} = 100$ TeV, $M_{X_1} = 50$ TeV, $\kappa_a = 10^{-14}$ GeV $^{-2}$. The horizontal dashed line corresponds to $\epsilon = \frac{\kappa_a}{16\pi} M_{X_2}^2$ and the diagonal dashed line corresponds to $\epsilon = \kappa_a T^2$. Note the kinematic suppression of $|\epsilon_1|$ at $T \lesssim M_{X_2}$.

parameters using the Cutkosky rules [34]. To find the CP violation in the equilibrium rates one must then take a thermal average:

$$\langle v(\sigma(ij \rightarrow kl) - \sigma(\bar{i}\bar{j} \rightarrow \bar{k}\bar{l})) \rangle = \frac{g_i g_j T}{8\pi^4 n_i^{eq} n_j^{eq}} \int_{(m_i+m_j)^2}^{\Lambda^2} p_{ij} E_i E_j v(\sigma - \bar{\sigma}) K_1 \left(\frac{\sqrt{\hat{s}}}{T} \right) d\hat{s}. \quad (3.22)$$

The results for such a calculation are depicted in figure 4. At high temperature $T \gg M_{X_2}$, one expects on dimensional grounds the CP symmetric thermally averaged cross section to scale as,

$$\langle \sigma v \rangle \sim \kappa^2 T^2, \quad (3.23)$$

where κ is the general scale of the relevant couplings. Similarly the CP violation is expected to scale as:

$$\epsilon \sim \kappa T^2. \quad (3.24)$$

Unlike the CP asymmetry in the decays, the CP asymmetries in the scatterings are temperature dependent. Note ϵ_1 is necessarily suppressed on kinematic grounds at low temperatures (W_1 does not depend on the heaviest particle mass, M_{X2} , while the CP violation is sensitive to M_{X2} from the on-shell particles in the loop). The other CP violating parameters take values close to

$$\epsilon \sim \frac{\kappa}{16\pi} M_{X2}^2, \quad (3.25)$$

at temperatures $T \ll M_{X2}$, as can be seen in figure 4.

4 Boltzmann equations

4.1 Differential equations

The simplifying approximation of Maxwell-Boltzmann statistics allows one to factor out the chemical potential from the overall reaction rate density. Let us define:

$$r_{\Psi i} \equiv \frac{n_{\Psi i}}{n_{\Psi i}^{eq}} = \text{Exp} \left(\frac{\mu_{\Psi}}{T} \right), \quad \bar{r}_{\Psi i} \equiv \frac{n_{\bar{\Psi} i}}{n_{\bar{\Psi} i}^{eq}} = \text{Exp} \left(\frac{\mu_{\bar{\Psi}}}{T} \right). \quad (4.1)$$

The non-equilibrium reaction rate for the process $ij \rightarrow kl$ is then given by: $W^{\text{neq}}(ij \rightarrow kl) = r_i r_j W(ij \rightarrow kl)$. The Boltzmann equations can then be conveniently expressed using this notation. The Boltzmann equation for n_{X1} is given by:^{2,3}

$$\begin{aligned} \frac{dn_{X1}}{dt} = & -3Hn_{X1} + \frac{1}{2}\Gamma_{1A}^{\text{th}} n_{X1}^{eq} \left[(\bar{r}_u r_d \bar{r}_d + r_u r_d r_d) - 2r_{X1} \right] + \Gamma_{2B}^{\text{th}} n_{X2}^{eq} \left[r_{X2} - r_{X1} \right] \\ & + W_1 \left[r_d r_d + \bar{r}_d \bar{r}_d - r_{X1} r_u - r_{X1} \bar{r}_u \right] + W_3 \left[r_{X2} r_u + r_{X2} \bar{r}_u - r_{X1} r_u - r_{X1} \bar{r}_u \right] \\ & + 2W_4 \left[r_d r_u + \bar{r}_d \bar{r}_u - r_{X1} r_d - r_{X1} \bar{r}_d \right] + 2W_6 \left[1 - r_{X1} r_{X1} \right] + W_8 \left[1 - r_{X2} r_{X1} \right] \\ & + \epsilon_3 W_3 \left[\bar{r}_d \bar{r}_d - r_d r_d + r_{X2} \bar{r}_u - r_{X2} r_u \right]. \end{aligned} \quad (4.2)$$

The Boltzmann equation for n_{X2} is given by:

$$\begin{aligned} \frac{dn_{X2}}{dt} = & -3Hn_{X2} + \frac{1}{2}\Gamma_{2A}^{\text{th}} n_{X2}^{eq} \left[((\bar{r}_u r_d \bar{r}_d + r_u r_d r_d) - 2r_{X2}) \right] + \Gamma_{2B}^{\text{th}} n_{X2}^{eq} \left[r_{X1} - r_{X2} \right] \\ & + W_2 \left[r_d r_d + \bar{r}_d \bar{r}_d - r_{X2} r_u - r_{X2} \bar{r}_u \right] + W_3 \left[r_{X1} r_u + r_{X1} \bar{r}_u - r_{X2} r_u - r_{X2} \bar{r}_u \right] \\ & + 2W_5 \left[r_d r_u + \bar{r}_d \bar{r}_u - r_{X2} r_d - r_{X2} \bar{r}_d \right] + 2W_7 \left[1 - r_{X2} r_{X2} \right] + W_8 \left[1 - r_{X2} r_{X1} \right] \\ & + \frac{1}{2}\epsilon_D \Gamma_{2A}^{\text{th}} n_{X2}^{eq} \left[(\bar{r}_u r_d \bar{r}_d - r_u r_d r_d) \right] + \epsilon_3 W_3 \left[r_d r_d - \bar{r}_d \bar{r}_d + r_{X1} r_u - r_{X1} \bar{r}_u \right]. \end{aligned} \quad (4.3)$$

²The decay rates which appear here are thermally averaged (see appendix B.3).

³We will see below that the three flavours of right chiral down type quarks have the same chemical potentials in the temperature ranges we are interested in. This allows us to set $r_d = r_s = r_b$ in the following equations.

The Boltzmann equation for the baryon-minus-lepton number, n_{B-L} , is given by:

$$\begin{aligned}
\frac{dn_{B-L}}{dt} = & -3Hn_{B-L} + \frac{1}{2}\Gamma_{1A}^{\text{th}}n_{X1}^{\text{eq}}\left[\overline{r_u r_d r_d} - r_u r_d r_d\right] + \frac{1}{2}\Gamma_{2A}^{\text{th}}n_{X2}^{\text{eq}}\left[\overline{r_u r_d r_d} - r_u r_d r_d\right] \\
& + W_1\left[r_{X1}\overline{r_u} - r_{X1}r_u + \overline{r_d r_d} - r_d r_d\right] + W_2\left[r_{X2}\overline{r_u} - r_{X2}r_u + \overline{r_d r_d} - r_d r_d\right] \\
& + 2W_4\left[r_{X1}\overline{r_d} - r_{X1}r_d + \overline{r_d r_u} - r_d r_u\right] + 2W_5\left[(r_{X2}\overline{r_d} - r_{X2}r_d + \overline{r_d r_u} - r_d r_u)\right] \\
& + \epsilon_3 W_3\left[r_{X1}\overline{r_u} + r_{X1}r_u - r_{X2}\overline{r_u} - r_{X2}r_u\right] \\
& + \frac{1}{2}\epsilon_D \Gamma_{2A}^{\text{th}}n_{X2}^{\text{eq}}\left[2r_{X2} - (\overline{r_u r_d r_d} + r_u r_d r_d)\right].
\end{aligned} \tag{4.4}$$

The terms proportional to ϵ_3 and ϵ_D are the source terms coming from scatterings and decays respectively. These lead to the generation of a baryon asymmetry once there is a departure from thermal equilibrium. Note we have used the unitarity conditions to express the source terms in a form in which one sees they are explicitly zero when all $r_{\psi_i} = 1$ (thermal equilibrium) [18]. The other terms are the washout terms: these drive the solutions back to the equilibrium values.

We use the standard change of variable to obtain the Boltzmann equations in a radiation dominated universe in terms of temperature using:

$$H = \left(\frac{8\pi^3}{90}\right)^{1/2} g_{\text{eff}}^{1/2} \frac{T^2}{M_{Pl}} = \frac{1}{2t}, \tag{4.5}$$

where g_{eff} counts the effective radiation degrees of freedom and $M_{Pl} \approx 1.22 \times 10^{19}$ GeV is the Planck mass [30]. The total entropy is conserved in the absence of first order phase transitions in a radiation dominated universe and hence it is useful to normalise number densities to the entropy density $Y_\psi \equiv n_\psi/s$. The entropy density is,

$$s = \frac{2\pi^2}{45} h_{\text{eff}} T^3, \tag{4.6}$$

where h_{eff} counts the entropic degrees of freedom [30]. The resulting differential equations are of the form,

$$\frac{dY_\psi}{dT} = -\left(\frac{\pi}{45}\right)^{1/2} \frac{M_{Pl} h_{\text{eff}}}{s^2 g_{\text{eff}}^{1/2}} \left(1 + \frac{T}{4g_{\text{eff}}} \frac{dg_{\text{eff}}}{dT}\right) C(\psi) \tag{4.7}$$

where $C(\psi)$ is the collision term for ψ , e.g. for $\psi = X_1$ it corresponds to the right hand side of eq. (4.2) excluding the expansion term proportional to H .

4.2 Chemical potentials

The chemical potentials of the quarks and leptons depend on the baryon and lepton asymmetries. Here we are interested in determining the chemical potentials of the right chiral up and down type quarks. We consider two regimes: above and below the electroweak phase transition. We approximate the transition to occur instantaneously at a temperature T_{EW} at which point we take the SU(2) sphalerons to have switched off and the SM quarks and leptons to have gained masses through the Higgs mechanism.

Field	Relativistic degrees of freedom	chemical potential
u	$6 \times N_u$	μ_u
d	$6 \times N_d$	μ_d
e	$2 \times N_e$	μ_e
ν	$1 \times N_\nu$	μ_ν

Table 1. SM fermionic fields and relativistic degrees of freedom for temperatures below the electroweak phase transition. We set $N_\nu = 3$ and use a simple step function in determining N_u , N_d and N_e .

Above T_{EW}

In determining the chemical potentials in terms of n_{B-L} in this regime one takes into account: (i) the SU(3) sphalerons, (ii) the SU(2) sphalerons, (iii) the SM Yukawa interactions, (iv) conservation of the weak hypercharge. The analysis is the same as for the usual leptogenesis [36]. The chemical potential of the right chiral up type quark is given by:

$$\mu_{uR} = -\frac{10}{79} \frac{n_{B-L}}{T^2}. \quad (4.8)$$

The right chiral down type quark chemical potential is given by:

$$\mu_{dR} = \frac{38}{79} \frac{n_{B-L}}{T^2}. \quad (4.9)$$

The baryon asymmetry is related to n_{B-L} :

$$n_B = \frac{28}{79} n_{B-L}. \quad (4.10)$$

The chemical potentials of the up and down type quarks are therefore determined in terms of n_{B-L} in this temperature regime. The final n_B in this temperature regime is used as an initial condition for the Boltzmann equations at lower temperatures.

Below T_{EW}

Below the electroweak phase transition the electroweak sphalerons have switched off and the weak hypercharge is no longer conserved. However, lepton number is now conserved and the overall electric charge must still vanish. The fermionic fields present are listed in table 1. The baryon number asymmetry is approximately given by [36]:

$$n_B = \frac{T^2}{6} B, \quad (4.11)$$

where $B = 2N_u\mu_u + 2N_d\mu_d$ and N_u (N_d) is the number of relativistic up (down) type quark flavours. The lepton number asymmetry is approximately given by [36]:

$$n_L = \frac{T^2}{6} L, \quad (4.12)$$

where $L = 2N_e\mu_e + 3\mu_\nu$ and N_e is the number of relativistic charged lepton generations. The chemical potentials are determined using the following constraints:

- Net electric charge vanishes. Once the temperature drops below the mass of a field its number density is very rapidly suppressed, if the field is in chemical equilibrium, as is the case for the SM fermions. We approximate this by only counting fields with mass below the temperature in contributing to the net charge of the plasma. This yields a constraint:

$$2N_u\mu_u - N_d\mu_d - N_e\mu_e = 0. \quad (4.13)$$

- Rapid interactions involving W boson exchange give the following relation:

$$\mu_u + \mu_e - \mu_d - \mu_\nu = 0. \quad (4.14)$$

- $Y_L \equiv n_L/s$ is constant after T_{EW} . This gives the constraint:

$$\mu_\nu = \frac{L - 2N_e\mu_e}{3}, \quad (4.15)$$

where L is computed using the lepton asymmetry Y_L at T_{EW} .

Combining these three constraints gives the up quark chemical potential:

$$\mu_u = \left\{ L + B \left[\frac{1}{3} + \frac{1}{2N_d} + \frac{1}{2N_e} \right] \right\} \times \left[1 + \frac{3N_u}{N_e} + \frac{N_u}{N_d} + 2N_u \right]^{-1}. \quad (4.16)$$

The down type chemical potential can neatly be expressed as:

$$\mu_d = \frac{B - 2N_u\mu_u}{2N_d}. \quad (4.17)$$

In this temperature regime the chemical potentials of the quarks can therefore be determined in terms of n_B and the net lepton number n_L at the sphaleron switch-off temperature.

4.3 Numerical solutions

We solve the Boltzmann equations numerically using Mathematica [37]. This involves evolving the three coupled ordinary differential equations from a suitably high temperature to a temperature at which the B violation is no longer effective. The initial temperature is chosen to be high enough so the $2 \leftrightarrow 2$ interaction rates are well above the expansion rate. The initial conditions correspond to equilibrium distributions for X_1 and X_2 and zero n_{B-L} .⁴ At the electroweak phase transition the sphalerons switch off and the lepton number remains constant. We then proceed to track n_B rather than n_{B-L} using the value of n_B obtained at T_{EW} as an initial condition.

Finally a dilution factor is applied to the final Y_B if the X_2 and X_1 particles are sufficiently long lived. This dilution factor comes about because the X_2 and X_1 can come to dominate the energy density of the early universe. The universe switches from a radiation to a matter dominated epoch until the X_2 and X_1 decay. The decays of these particles then produces a large amount of entropy — slowing down the rate at which the universe is cooling

⁴Any initial $B - L$ would be erased by the on-shell interactions involving the new particles at the UV completion scale — even below this scale the effective $2 \leftrightarrow 2$ interactions are rapid enough to make the analysis independent of initial conditions so long as the post-inflation reheating temperature of the universe is sufficiently high.

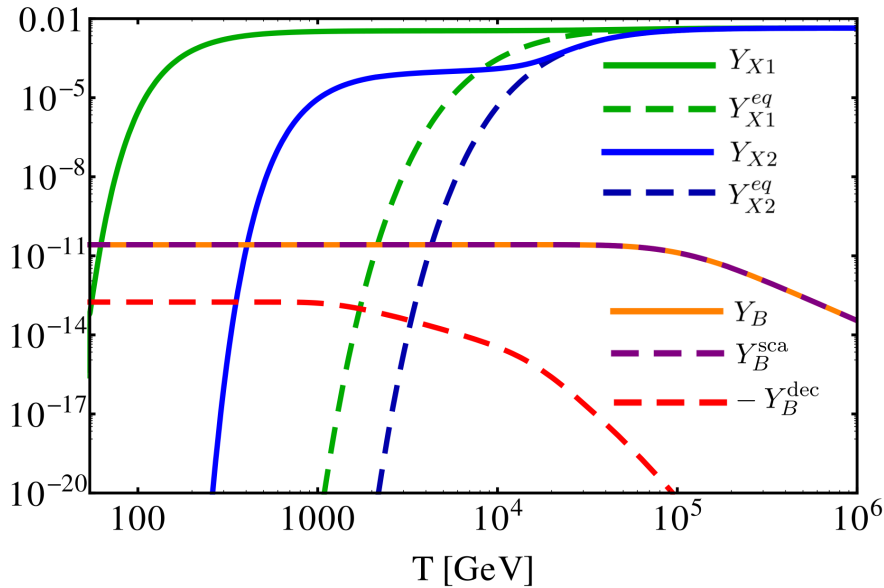


Figure 5. Example solution to the Boltzmann equations with $M_{X_2} = 100$ TeV, $M_{X_1} = 50$ TeV, all $\kappa_a = 10^{-16}$ GeV $^{-2}$ and number densities expressed in ratios to entropy $Y_\Psi \equiv n_\Psi/s$. The baryon asymmetry with CP violation only in scatterings (decays) Y_B^{sca} (Y_B^{dec}) is also shown. CP violating scatterings are the dominant asymmetry generation mechanism in this example.

— and lead to a departure from the assumption of constant entropy in the early universe. The dilution factor can be approximated as [38]:

$$d_S = \text{Max} \left[1.8 h_{\text{eff}}^{1/4} \frac{Y_\alpha|_{T_{\text{fo}}}}{(\Gamma_\alpha M_{Pl})^{1/2}}, 1 \right], \quad (4.18)$$

where $Y_\alpha|_{T_{\text{fo}}}$ is the density to entropy ratio of the decaying particle at freeze out and Γ_α is its decay rate. Being more abundant at freezeout and having a longer lifetime X_1 tends to dominate the dilution factor.

An example solution to the Boltzmann equations is shown in figure 5. The cosmological history of the universe proceeds in the following way. At high temperature the $2 \leftrightarrow 2$ interactions are rapid, keeping the n_{X_1} and n_{X_2} close to their equilibrium values. Due to the expansion of the universe the particles are never exactly in equilibrium. As the temperature decreases the interaction rates drop and r_{X_1} , r_{X_2} and Y_B continue to increase. The size of the source term will depend not only on the CP violation but also on how far away the temperature is from M_{X_2} and M_{X_1} : in the massless limit $r_{X_1} = r_{X_2} = 1$ even in the absence of interactions (assuming a common T). Eventually, at $\Gamma_\alpha \sim H$, the decays take over. Excess X_2 and X_1 decay away and the X_2 decays also contribute to the baryon asymmetry. The freezeout temperature is determined by the coupling size; numerically we find the maximum asymmetry for freezeout at $T \sim M_\alpha$, i.e. before the number densities of X_1 and X_2 become Boltzmann suppressed.

The CP violation in the decays and the scatterings increases $\sim \kappa$. However, as κ increases the freeze out of the $2 \leftrightarrow 2$ interactions occurs closer and closer to the decay temperature, i.e. at $\Gamma_\alpha \sim H$, and the particles are kept closer to thermal equilibrium. The

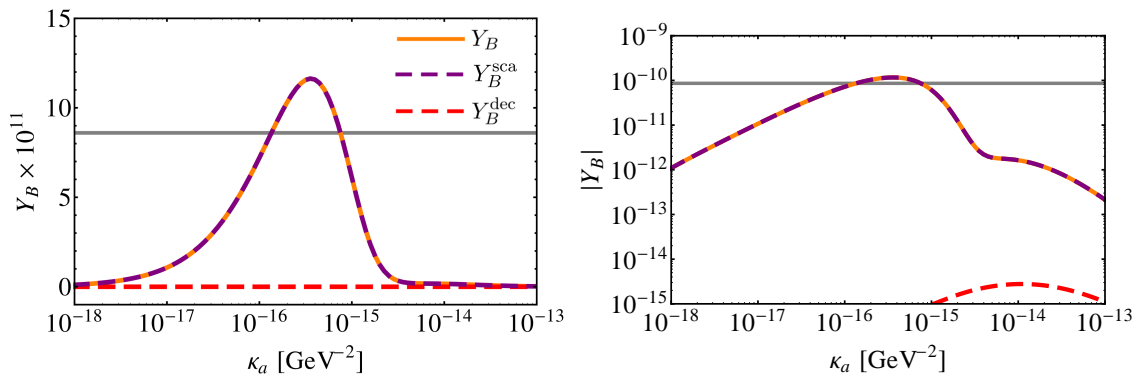


Figure 6. *Left:* the final baryon asymmetry as a function of the couplings (all set equal) κ_a , the masses have been set to $M_{X_2} = 100$ TeV and $M_{X_1} = 90$ TeV. The observed value of the baryon asymmetry is indicated by a gray horizontal line and is reached for couplings in the range $10^{-16} \text{ GeV}^{-2} \lesssim \kappa_a \lesssim 10^{-15} \text{ GeV}^{-2}$. Also shown are the final asymmetries Y_B^{sca} (Y_B^{dec}) calculated with CP violation only in the scatterings (decays). *Right:* same as in the left plot but on a double logarithmic scale.

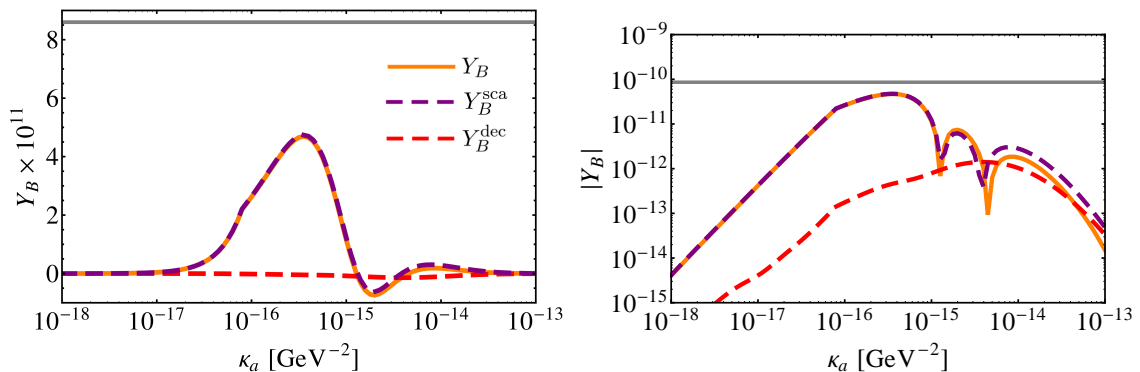


Figure 7. Same as in figure 6 but with $M_{X_1} = 50$ TeV. The decays now play a more significant role but the final baryon asymmetry cannot match the observed value for any choice of couplings κ_a .

resulting effect on Y_B is shown in figures 6 – 8 in which the final asymmetry first increases as the couplings increase but eventually becomes suppressed.

Also shown in figures 6 – 8 is the domination of the CP violating scatterings in determining the final Y_B for the majority of the parameter space. This is because the CP violation due to the scatterings — which scales as κT^2 — can be relatively high at the freezeout temperature. This balances the relatively small departure from equilibrium just prior to freezeout, when the $2 \leftrightarrow 2$ interactions generate the majority of the asymmetry, compared with the departure from equilibrium at $\Gamma_2 \sim H$, when the decays contribute to the asymmetry. The CP violation in the decays is typically much smaller than the CP violation in the scatterings at freeze out — at least for couplings small enough for a significant departure from equilibrium to take place. As M_{X_1} is decreased the CP violation in decays becomes more important. The reasons are twofold: smaller M_{X_1} results in a greater $|\epsilon_D|$ and in larger washout effects after X_2 freezes out for kinematic reasons.

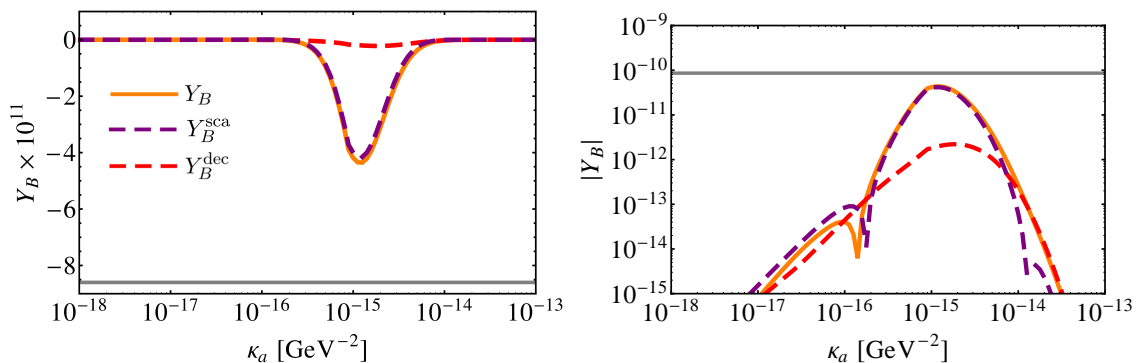


Figure 8. Same as in figure 6 but with $M_{X_1} = 10$ TeV. Note the sign of the asymmetry can be changed by changing the sign of the CP violating phase. The horizontal gray line now indicates the magnitude of the observed asymmetry but with opposite sign. The CP violation in the decays is now close to maximal but the scatterings still dominate for $\kappa_a \lesssim 10^{-14}$ GeV $^{-2}$.

Note that the scaling of the CP violation with temperature is different in leptogenesis. The dimensionless couplings in leptogenesis mean the CP violation in scatterings will not grow as strongly with temperature, as it does here, but remain mostly constant [24–28]. This explains why the CP violating scatterings can play a crucial role in the neutron portal but only a negligible role in resonant leptogenesis in determining the final Y_B [24].

The precision of these calculations can be improved by taking into account departures from kinetic equilibrium, quantum statistics and thermal masses [39–43]. The corrections are expected to be at most $\mathcal{O}(1)$, as in the case for leptogenesis. We leave the inclusion of such effects to further work.

5 Constraints

Constraints on the neutron portal have previously been discussed in ref. [29]. The decay of relic particles after $t \sim 1$ s can disrupt big bang nucleosynthesis (BBN) [44–46]. Considering the X_1 lifetime one finds a constraint [29]:

$$\kappa_1 \gtrsim \left(\frac{1 \text{ TeV}}{M_{X_1}} \right)^{5/2} 10^{-18} \text{ GeV}^{-2}. \quad (5.1)$$

Similarly from the X_2 lifetime one requires [29]:

$$\kappa_2 \text{ or } \kappa_3 \gtrsim \left(\frac{1 \text{ TeV}}{M_{X_2}} \right)^{5/2} 10^{-18} \text{ GeV}^{-2}, \quad (5.2)$$

where we have ignored the final state M_{X_1} mass. The κ_3 bound becomes more stringent as M_{X_1} is increased.

Operators of the form $\kappa \overline{X_{\alpha L}} d_R \overline{u_R^c} d_R$ or $\kappa \overline{X_{\alpha L}} d_R \overline{Q_L^c} Q_L$, where X_α is Majorana, are constrained by limits on neutron-antineutron oscillations (see figure 9). The oscillation period is estimated as [29],

$$\tau_{n-\bar{n}} \sim 3 \times 10^8 \text{ s} \times \left(\frac{M_{X_\alpha}}{1 \text{ TeV}} \right) \left(\frac{10^{-13} \text{ GeV}^{-2}}{\kappa} \right)^2 \left(\frac{250 \text{ MeV}}{\Lambda_{QCD}} \right)^6, \quad (5.3)$$

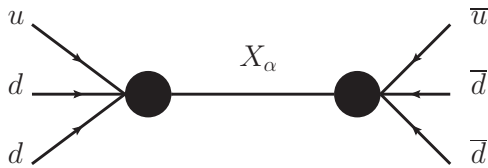


Figure 9. Neutron-antineutron oscillation induced by operators of the form $\kappa \overline{X_{\alpha L}} d_R \overline{u_R^c} d_R$ or $\kappa \overline{X_{\alpha L}} d_R \overline{Q_L^c} Q_L$.

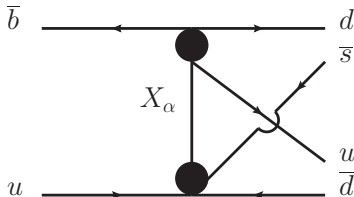


Figure 10. Meson decay $B^+ \rightarrow \pi^+ K^0$ due to the operators $\kappa \overline{X_{\alpha L}} u_R \overline{s_R^c} b_R + \kappa \overline{X_{\alpha L}} u_R \overline{s_R^c} d_R$.

where we have approximated the nuclear matrix element with Λ_{QCD} . Comparison to the experimental limit from bound neutrons $\tau_{n-\bar{n}} \geq 2.4 \times 10^8$ s [47] (or from free neutrons $\tau_{n-\bar{n}} \geq 8.6 \times 10^7$ s [48] — which has smaller theoretical uncertainty) shows broad compatibility in the parameter range of interest. The operators we considered, however, couple only off-diagonally in down quark flavour. The oscillation period is therefore further suppressed and certainly does not pose any problems for the parameter choices we have been interested in above. Similar conclusions hold for the loop induced meson mixing operators [29].

Flavour off-diagonal operators such as $\kappa \overline{X_{\alpha L}} u_R \overline{s_R^c} b_R + \kappa \overline{X_{\alpha L}} u_R \overline{s_R^c} d_R$ will lead to meson decays such as $B^+ \rightarrow \pi^+ K^0$ (see figure 5). The contribution to the branching ratio is estimated as:

$$Br_X(B^+ \rightarrow \pi^+ K^0) \approx 10^{-38} \times \left(\frac{1 \text{ TeV}}{M_{X_\alpha}} \right)^4 \left(\frac{\kappa}{10^{-12} \text{ GeV}^{-2}} \right)^4 \quad (5.4)$$

which is far below the experimental observation $Br(B^+ \rightarrow \pi^+ K^0) = (2.3 \pm 0.07) \times 10^{-5}$ [49–51]. The most important constraints on this scenario therefore come from BBN and neutron-antineutron oscillations.

6 UV completions

One or more complex scalars transforming as $S_\rho \sim (3, 1, 4/3)$ under the SM gauge group may be added in order to UV complete this model. The high energy interaction Lagrangian takes the form:

$$\Delta \mathcal{L} = y_{\rho \alpha i} S_\rho^* \overline{X_{\alpha L}} u_{Ri} + \lambda_{\rho ij} S_\rho \overline{d_{Ri}^c} d_{Rj} + H.c., \quad (6.1)$$

where $y_{\rho \alpha i}$ and $\lambda_{\rho ij}$ are dimensionless couplings and the latter is antisymmetric in quark flavour. For couplings $y_{\rho \alpha i} \sim \lambda_{\rho ij} \sim \mathcal{O}(1)$ the effective operators of eq. (3.1) are generated with $\kappa \sim 1/M_{S_\rho}^2$, where M_{S_ρ} is the mass of the scalar S_ρ , once the S_ρ are integrated out.

If the couplings are only to the u , s and b quarks two copies of S_ρ must be added in order to obtain complex phases. However, in a realistic model — allowing couplings to all possible quarks — one finds two complex phases with only one S_ρ . The corresponding 28 complex phases of the low energy effective field theory are therefore not independent. This can lead to cancellations of phases in some of the interference terms and may reduce the overall CP violation. We leave investigation of such effects to further work.

If we do not impose a global lepton number symmetry the X_α will mix with the SM neutrino degrees-of-freedom through Yukawa couplings of the form $\epsilon_{ab}\overline{l_{La}}\Phi_b^*X_{\alpha L}^c$, where ϵ_{ab} is the Levi-Civita symbol, Φ is the SM Higgs doublet and l_L the SM lepton doublet. If the X_α are to be responsible for the observed neutrino masses, the mixing between the mostly-active light neutrinos and mostly-sterile heavy states must be of the order $\theta \sim \sqrt{m_\nu/M_{X_\alpha}}$, where m_ν is the light neutrino mass. Consequently S_ρ mediated proton decay $p \rightarrow K^+\nu$ will occur with a partial lifetime estimated as:

$$\tau_{p \rightarrow K^+\nu} \sim \frac{10^{13} \text{ years}}{|y_{\rho\alpha u}\lambda_{\rho ds}|^2} \left(\frac{250 \text{ MeV}}{\Lambda_{QCD}}\right)^5 \left(\frac{0.05 \text{ eV}}{m_\nu}\right) \left(\frac{M_{X_\alpha}}{10 \text{ TeV}}\right) \left(\frac{M_{S_\rho}}{10^7 \text{ GeV}}\right)^4. \quad (6.2)$$

The partial proton lifetime will conflict with the experimental limit $\tau_{p \rightarrow K^+\nu} \gtrsim 2.3 \times 10^{33}$ years [52] for the parameter range of interest if the X_α are responsible for the neutrino mass through the usual seesaw mechanism.

Furthermore Yukawa couplings of the form $\epsilon_{ab}\overline{l_{La}}\Phi_b^*X_{\alpha L}^c$ would lead to leptogenesis style interactions and subsequent complications in the analysis of the cosmological history. The non-zero neutrino masses can be explained, even with the global lepton number symmetry we have imposed, by introducing right chiral singlets N_R with Yukawa couplings $\epsilon_{ab}\overline{l_{La}}\Phi_b^*N_R$: these give the SM neutrinos Dirac masses once the SM Higgs gains a vacuum expectation value. Majorana masses for the N_R are, of course, forbidden.

In this section we have briefly discussed UV completions for the the neutron portal effective operators of section 3. Other neutron portal type operators are possible and we note that similar conclusions for their UV completions, in particular regarding proton decay if no global lepton number conservation is imposed, also hold.

7 Conclusion

We have studied the effects of CP violation in $2 \leftrightarrow 2$ interactions for baryogenesis. As a case study we have taken a neutron portal model in which two Majorana fermions X_1 and X_2 are coupled to the neutron operator. In order to find the final baryon asymmetry, we calculated all the relevant decay rates and $2 \leftrightarrow 2$ scattering rates and solved the Boltzmann evolution equations numerically. From dimensional grounds the CP violation in the decays scales as $\kappa M_{X_2}^2$ where κ is the order-of-magnitude of the relevant couplings. The CP violation in the scatterings scales as $\kappa M_{X_2}^2$ at low temperatures but grows as κT^2 for $T \gg M_X$. Consequently CP violating $2 \leftrightarrow 2$ scatterings can play a crucial role at high temperature even when the departure-from-equilibrium is relatively small. Indeed for many areas of the parameter space the CP violating scatterings play a dominant role in determining the final baryon asymmetry. This is to be contrasted with leptogenesis — in which the CP violating scatterings do not scale as strongly with temperature — and have only a negligible effect on the final asymmetry [24–28]. We also discussed constraints on the model from experiments and BBN and discussed possible UV completions. The techniques learned can be applied

to other baryogenesis scenarios in order to take into account the — possibly dominant — corrections due to CP violating scatterings.

Acknowledgments

IB and AM were supported by the Commonwealth of Australia. NFB and RRV were supported in part by the Australian Research Council. KP was supported by the Netherlands Foundation for Fundamental Research of Matter (FOM) and the Netherlands Organisation for Scientific Research (NWO). Feynman diagrams drawn using Jaxodraw [53].

A Unitarity constraint for multiple quark generations

Here we discuss the unitarity constraint in the case of couplings to all possible quark flavours and show that at least two X_α are required to obtain a non-zero source term from the CP violating scatterings.⁵ We denote the equilibrium reaction rates as:

$$W(X_\alpha + d_i \rightarrow \bar{u}_j + \bar{d}_k) = (1 + \epsilon_{\alpha ijk})W_{\alpha ijk}, \quad (\text{A.1})$$

$$W(X_\alpha + d_i \rightarrow X_\beta + d_j) = (1 + \zeta_{\alpha i\beta j})Z_{\alpha i\beta j}, \quad (\text{A.2})$$

$$W(u_i + d_j \rightarrow u_k + d_l) = (1 + a_{ijkl})A_{ijkl}, \quad (\text{A.3})$$

where the CP conjugate can be found by taking $\epsilon_{\alpha ijk} \rightarrow -\epsilon_{\alpha ijk}$, $\zeta_{\alpha i\beta j} \rightarrow -\zeta_{\alpha i\beta j}$ or $a_{ijkl} \rightarrow -a_{ijkl}$. Note we have also included quark flavour changing interactions in order to make the argument more general. The unitarity constraint then yields:

$$\sum_{\beta j} \zeta_{\alpha i\beta j} Z_{\alpha i\beta j} + \sum_{jk} \epsilon_{\alpha ijk} W_{\alpha ijk} = 0, \quad (\text{A.4})$$

$$\sum_{ml} a_{jkml} A_{jkml} + \sum_{\alpha i} \epsilon_{\alpha ijk} W_{\alpha ijk} = 0. \quad (\text{A.5})$$

Now consider the case of only one Majorana $X_\alpha = X_1$. (The argument may be easily modified for Dirac X_1 and the conclusions remain unchanged.) Taking $r_d = r_s = r_b$ and $r_u = r_c = r_t$ the Boltzmann equation for the baryon asymmetry (excluding the decay terms) is:

$$\frac{dn_B}{dt} + 3Hn_B = \sum_{ijk} W_{1ijk} \left[(1 - \epsilon_{1ijk})(\bar{r}_d \bar{r}_u + r_{X1} \bar{r}_d) - (1 + \epsilon_{1ijk})(r_d r_u + r_{X1} r_d) \right]. \quad (\text{A.6})$$

Now consider only the source term:

$$- \sum_{ijk} \epsilon_{1ijk} W_{1ijk} \left[\bar{r}_d \bar{r}_u + r_{X1} \bar{r}_d + r_d r_u + r_{X1} r_d \right]. \quad (\text{A.7})$$

A departure from equilibrium due to the expansion of the universe gives $r_{X1} \neq 1$ and $r_u = r_d = \bar{r}_u = \bar{r}_d = 1$ and the source term may be written:

$$- (2 + 2r_X) \sum_i \sum_{jk} \epsilon_{1ijk} W_{1ijk} = (2 + 2r_X) \sum_i \sum_j \zeta_{1i1j} Z_{1i1j} = 0, \quad (\text{A.8})$$

where the first equality follows from eq. (A.4) and the second as $\zeta_{\alpha i\alpha j} = -\zeta_{\alpha j\alpha i}$. Hence the generation of an asymmetry from scatterings with only a single X_α is not possible.

⁵For clarity, we only consider initial states $X_\alpha + d_i$ here; the arguments can easily be generalised to include $X_\alpha + u_i$ initial states.

B Cross sections, decay rates and CP violation

B.1 Cross sections

Here we collect the results of our calculations for the cross sections used in the above analysis. The sums over initial and final colours have been performed. The cross sections have been calculated in the centre-of-mass frame. E_a and E_b (E_c and E_d) denote initial (final) state energies of the particles in the order listed. The initial momentum is denoted p_i and the final momentum p_f . The centre-of-mass energy is $\sqrt{\hat{s}}$.

$$u + X_\alpha \rightarrow \bar{s} + \bar{b}$$

$$E_a E_b \sigma v = \frac{3|\kappa_\alpha|^2 p_f}{2\pi\sqrt{\hat{s}}} [E_a E_b + p_i^2] [E_c E_d + p_f^2] \quad (\text{B.1})$$

$$s + X_\alpha \rightarrow \bar{u} + \bar{b}$$

$$E_a E_b \sigma v = \frac{3|\kappa_\alpha|^2 p_f}{2\pi\sqrt{\hat{s}}} \left[E_a E_b E_c E_d + \frac{1}{3} p_i^2 p_f^2 \right] \quad (\text{B.2})$$

$$X_2 + \bar{u} \rightarrow X_1 + \bar{u}$$

$$E_a E_b \sigma v = \frac{3|\kappa_3|^2 p_f}{8\pi\sqrt{\hat{s}}} \left[2E_a E_b E_c E_d + E_c E_d p_i^2 + E_a E_b p_f^2 + \frac{4}{3} p_i^2 p_f^2 + \frac{\text{Re}[\kappa_3 \kappa_3]}{|\kappa_3|^2} M_{X_2} M_{X_1} E_b E_d \right] \quad (\text{B.3})$$

$$X_2 + X_1 \rightarrow \bar{u} u$$

$$E_a E_b \sigma v = \frac{3|\kappa_3|^2 p_f}{16\pi\sqrt{\hat{s}}} \left[2E_a E_b E_c E_d + \frac{2}{3} p_i^2 p_f^2 - \frac{\text{Re}[\kappa_3 \kappa_3]}{|\kappa_3|^2} M_{X_2} M_{X_1} (E_c E_d + p_f^2) \right] \quad (\text{B.4})$$

$$X_\alpha + X_\alpha \rightarrow \bar{u} u$$

$$E_a E_b \sigma v = \frac{3|\kappa_{\alpha+3}|^2 p_f}{16\pi\sqrt{\hat{s}}} \left[2E_a E_b E_c E_d + \frac{2}{3} p_i^2 p_f^2 - M_{X_\alpha}^2 (E_c E_d + p_f^2) \right]. \quad (\text{B.5})$$

B.2 Cross sections — CP violation

CP violation for $u_R + X_1 \rightarrow u_R + X_2$:

This CP violation arises from the interference of two tree level diagrams (corresponding to different continuous fermion lines) with a loop level diagram.

$$E_a E_b (\sigma - \bar{\sigma}) v = \frac{3p_f}{\pi\sqrt{\hat{s}}} g_1(\hat{s}, m_s, m_b) \left\{ 2\text{Im}[\kappa_3 \kappa_1 \kappa_2^*] [E_a E_b + p_i^2] [E_c E_d + p_f^2] + \text{Im}[\kappa_3^* \kappa_1 \kappa_2^*] M_{X_1} M_{X_2} E_b E_d \right\}, \quad (\text{B.6})$$

where:

$$g_1(\hat{s}, m_i, m_j) = \frac{1}{32\pi} \left[\hat{s} - (m_i^2 + m_j^2) \right] \sqrt{1 - \frac{2(m_i^2 + m_j^2)}{\hat{s}} + \frac{(m_i^2 - m_j^2)^2}{\hat{s}^2}}. \quad (\text{B.7})$$

CP violation for $u_R + X_{1L} \rightarrow \bar{s} + \bar{b}$:

This CP violation arises from the interference of a tree level diagram with two different loop level diagrams.

$$E_a E_b (\sigma - \bar{\sigma}) v = \frac{6p_f}{\pi\sqrt{\hat{s}}} \text{Im}[\kappa_1^* \kappa_2 \kappa_3^*] g_1(\hat{s}, m_u, M_{X2}) \left[E_a E_b + p_i^2 \right] \left[E_c E_d + p_f^2 \right] - \frac{3p_f}{\pi\sqrt{\hat{s}}} \text{Im}[\kappa_1^* \kappa_2 \kappa_3] E_b g_2(\hat{s}, m_u, M_{X2}) M_{X1} M_{X2} \left[E_c E_d + p_f^2 \right], \quad (\text{B.8})$$

where:

$$g_2(\hat{s}, m_i, m_j) = -\frac{1}{32\pi\sqrt{\hat{s}}} \left[\hat{s} + m_i^2 - m_j^2 \right] \sqrt{1 - \frac{2(m_i^2 + m_j^2)}{\hat{s}} + \frac{(m_i^2 - m_j^2)^2}{\hat{s}^2}}. \quad (\text{B.9})$$

CP violation for $u_R + X_2 \rightarrow \bar{s}_R + \bar{b}_R$:

This CP violation arises from the interference of a tree level diagram with two different loop level diagrams.

$$E_a E_b (\sigma - \bar{\sigma}) v = \frac{6p_f}{\pi\sqrt{\hat{s}}} \text{Im}[\kappa_2^* \kappa_1 \kappa_3] g_1(\hat{s}, m_u, M_{X1}) \left[E_a E_b + p_i^2 \right] \left[E_c E_d + p_f^2 \right] - \frac{3p_f}{\pi\sqrt{\hat{s}}} \text{Im}[\kappa_2^* \kappa_1 \kappa_3^*] E_b g_2(\hat{s}, m_u, M_{X1}) M_{X1} M_{X2} \left[E_c E_d + p_f^2 \right]. \quad (\text{B.10})$$

B.3 Decay rates

The decay rates which appear in the Boltzmann equations are thermally averaged [27]:

$$\Gamma^{\text{th}} = \frac{K_1(M/T)}{K_2(M/T)} \Gamma, \quad (\text{B.11})$$

where M is the mass of the decaying particle, Γ is the decay rate in the rest frame of the decaying particle and $K_n(x)$ is the modified Bessel function of the second kind of order n .

$\Gamma(X_{1L} \rightarrow usb)$

Ignoring the final state masses the decay width is:

$$\frac{\Gamma_{1A}}{2} = \frac{|\kappa_1|^2 M_{X1}^5}{1024\pi^3}, \quad (\text{B.12})$$

so Γ_{1A} is the sum over the partial widths $\Gamma(X_{1L} \rightarrow usb) + \Gamma(X_{1L} \rightarrow \overline{usb})$.

$\Gamma(X_2 \rightarrow usb)$

Ignoring the final state masses the decay width is:

$$\frac{\Gamma_{2A}}{2} = \frac{|\kappa_2|^2 M_{X2}^5}{1024\pi^3}, \quad (\text{B.13})$$

so Γ_{2A} is the sum over the partial widths $\Gamma(X_2 \rightarrow usb) + \Gamma(X_2 \rightarrow \overline{usb})$.

$\Gamma(X_2 \rightarrow X_1 L u \bar{u})$

For this decay we take into account the mass of X_1 . In integral form the width is given by:

$$\Gamma_{X_2 B} = \frac{3|\kappa_3|^2 M_{X_2}^5}{512\pi^3} \int dx_a \int dx_b \left\{ x_a(1 + \mu_{12} - x_a) + x_b(1 - \mu_{12} - x_b) + \frac{2\text{Re}[\kappa_3^2] M_{X_1}}{|\kappa_3|^2 M_{X_2}} (1 - \mu_{12} - x_b) \right\}, \quad (\text{B.14})$$

where $\mu_{12} \equiv (M_{X_1}/M_{X_2})^2$ and the limits of integration are:

$$\frac{1}{2} \left([2 - x_a] - \sqrt{x_a^2 - 4\mu_{12}} \right) \leq x_b \leq \frac{1}{2} \left([2 - x_a] + \sqrt{x_a^2 - 4\mu_{12}} \right), \quad (\text{B.15})$$

$$2\sqrt{\mu_{12}} \leq x_a \leq 1 + \mu_{12}. \quad (\text{B.16})$$

B.4 CP violation in the X_2 decay

This CP violation arises from the interference of a tree level diagram with two different loop level diagrams. The tree level amplitude for $X_2 \rightarrow usb$ with momenta p_i, p_a, p_b, p_c respectively is given by:

$$\mathcal{M}_T = -i\kappa_2^* \left[\bar{u}(p_a) L u(p_i) \right] \left[\bar{u}(p_c) L v(p_b) \right]. \quad (\text{B.17})$$

Here L (R) denotes the left (right) projection operator. The first loop diagram has amplitude:

$$\mathcal{M}_{L1} = \kappa_3^* \kappa_1^* \left[\bar{u}(p_a) L u(p_i) \right] \left[\bar{u}(p_c) L v(p_b) \right] \int \frac{d^4 k}{(2\pi)^4} \frac{\text{Tr} \left[R (\not{p}_t + \not{k}) \not{k} \right]}{\left([p_t + k]^2 - M_{X_1}^2 \right) \left(k^2 - m_u^2 \right)}, \quad (\text{B.18})$$

where $p_t = p_i - p_a$. The second loop diagram has amplitude:

$$\mathcal{M}_{L2} = \kappa_1^* \kappa_3 M_{X_1} \left[\bar{u}(p_c) L v(p_b) \right] \int \frac{d^4 k}{(2\pi)^4} \frac{\left[\bar{v}(p_i) R \not{k} v(p_a) \right]}{\left([p_t + k]^2 - M_{X_1}^2 \right) \left(k^2 - m_u^2 \right)}. \quad (\text{B.19})$$

The total CP violation can be expressed as:

$$\epsilon_D = \gamma_1 + \gamma_2, \quad (\text{B.20})$$

where γ_1 (γ_2) comes from the interference between \mathcal{M}_T^* and \mathcal{M}_{L1} (\mathcal{M}_{L2}).

Contribution from $\mathcal{M}_T^* \mathcal{M}_{L1}$

$$\gamma_1 \Gamma_{2A} = 3\text{Im}[\kappa_2 \kappa_1^* \kappa_3^*] \frac{M_{X_2}^5}{512\pi^4} \int_0^{1-\mu_{12}} dx_a x_a^2 (1 - x_a) g_3 \left(\frac{M_{X_2} x_a}{2} \right), \quad (\text{B.21})$$

where,

$$g_3(E) = \int_{-1}^1 dc_\theta \frac{x_0(x_0^2 + x_0 \sqrt{x_0^2 + E^2 - 2x_0 E c_\theta + M_{X_1}^2} - x_0 E c_\theta)}{\sqrt{x_0^2 + E^2 - 2x_0 E c_\theta + M_{X_1}^2} + x_0 - E c_\theta} \quad (\text{B.22})$$

and

$$x_0 = \frac{(M_{X_2}^2 - 2M_{X_2} E - M_{X_1}^2)}{2(M_{X_2} - E - E c_\theta)}. \quad (\text{B.23})$$

Contribution from $\mathcal{M}_T^* \mathcal{M}_{L2}$

$$\gamma_2 \Gamma_{2A} = 3 \text{Im}[\kappa_2 \kappa_1^* \kappa_3] \frac{M_{X1} M_{X2}^4}{512 \pi^4} \int_0^{1-\mu_{12}} dx_a x_a (1-x_a) g_4 \left(\frac{M_{X2} x_a}{2} \right), \quad (\text{B.24})$$

where,

$$g_4(E) = \int_{-1}^1 dc_\theta \frac{x_0^2 E (1 + c_\theta)}{(x_0^2 - 2x_0 E c_\theta + E^2 + M_{X1}^2)^{1/2} + x_0 - E c_\theta}, \quad (\text{B.25})$$

and the expression for x_0 is given in eq. (B.23).

References

- [1] H.-Y. Chiu, *Symmetry between particle and antiparticle populations in the universe*, *Phys. Rev. Lett.* **17** (Sep, 1966) 712–714.
- [2] **WMAP** Collaboration, G. Hinshaw et al., *Nine-Year Wilkinson Microwave Anisotropy Probe (WMAP) Observations: Cosmological Parameter Results*, *Astrophys. J. Suppl.* **208** (2013) 19, [[arXiv:1212.5226](#)].
- [3] **Planck** Collaboration, P. Ade et al., *Planck 2013 results. XVI. Cosmological parameters*, [[arXiv:1303.5076](#)].
- [4] C. J. Copi, D. N. Schramm, and M. S. Turner, *Big bang nucleosynthesis and the baryon density of the universe*, *Science* **267** (1995) 192–199, [[astro-ph/9407006](#)].
- [5] A. Sakharov, *Violation of CP Invariance, c Asymmetry, and Baryon Asymmetry of the Universe*, *Pisma Zh. Eksp. Teor. Fiz.* **5** (1967) 32–35.
- [6] S. Weinberg, *Cosmological Production of Baryons*, *Phys. Rev. Lett.* **42** (1979) 850–853.
- [7] E. W. Kolb and S. Wolfram, *Baryon Number Generation in the Early Universe*, *Nucl. Phys. B* **172** (1980) 224.
- [8] J. N. Fry, K. A. Olive, and M. S. Turner, *Hierarchy of cosmological baryon generation*, *Phys. Rev. Lett.* **45** (Dec, 1980) 2074–2077.
- [9] M. Fukugita and T. Yanagida, *Baryogenesis Without Grand Unification*, *Phys. Lett. B* **174** (1986) 45.
- [10] L. Bento and Z. Berezhiani, *Leptogenesis via collisions: The Lepton number leaking to the hidden sector*, *Phys. Rev. Lett.* **87** (2001) 231304, [[hep-ph/0107281](#)].
- [11] A. Hook, *Unitarity constraints on asymmetric freeze-in*, *Phys. Rev. D* **84** (2011) 055003, [[arXiv:1105.3728](#)].
- [12] J. Unwin, *Towards Cogenesis via Asymmetric Freeze-in: The χ Who Came-in from the Cold*, [[arXiv:1406.3027](#)].
- [13] Y. Cui, L. Randall, and B. Shuve, *A WIMPy Baryogenesis Miracle*, *JHEP* **1204** (2012) 075, [[arXiv:1112.2704](#)].
- [14] N. Bernal, F.-X. Josse-Michaux, and L. Ubaldi, *Phenomenology of WIMPy baryogenesis models*, *JCAP* **1301** (2013) 034, [[arXiv:1210.0094](#)].
- [15] N. Bernal, S. Colucci, F.-X. Josse-Michaux, J. Racker, and L. Ubaldi, *On baryogenesis from dark matter annihilation*, *JCAP* **1310** (2013) 035, [[arXiv:1307.6878](#)].
- [16] J. Kumar and P. Stengel, *WIMPy Leptogenesis With Absorptive Final State Interactions*, *Phys. Rev. D* **89** (2014) 055016, [[arXiv:1309.1145](#)].

- [17] J. Racker and N. Rius, *Helicitogenesis: WIMPy baryogenesis with sterile neutrinos and other realizations*, [[arXiv:1406.6105](#)].
- [18] I. Baldes, N. F. Bell, K. Petraki, and R. R. Volkas, *Particle-antiparticle asymmetries from annihilations*, *Phys. Rev. Lett.* **113** (2014) 181601, [[arXiv:1407.4566](#)].
- [19] S. Nussinov, *Technoc cosmology: could a technibaryon excess provide a ‘natural’ missing mass candidate?*, *Phys. Lett.* **B 165** (1985) 55.
- [20] H. Davoudiasl and R. N. Mohapatra, *On Relating the Genesis of Cosmic Baryons and Dark Matter*, *New J. Phys.* **14** (2012) 095011, [[arXiv:1203.1247](#)].
- [21] K. Petraki and R. R. Volkas, *Review of asymmetric dark matter*, *Int. J. Mod. Phys.* **A 28** (2013) 1330028, [[arXiv:1305.4939](#)].
- [22] K. M. Zurek, *Asymmetric Dark Matter: Theories, Signatures, and Constraints*, *Phys. Rept.* **537** (2014) 91–121, [[arXiv:1308.0338](#)].
- [23] G. R. Farrar and G. Zaharijas, *Dark matter and the baryon asymmetry*, *Phys. Rev. Lett.* **96** (2006) 041302, [[hep-ph/0510079](#)].
- [24] A. Pilaftsis and T. E. J. Underwood, *Resonant leptogenesis*, *Nucl. Phys.* **B 692** (2004) 303–345, [[hep-ph/0309342](#)].
- [25] A. Pilaftsis and T. E. J. Underwood, *Electroweak-scale resonant leptogenesis*, *Phys. Rev.* **D 72** (2005) 113001, [[hep-ph/0506107](#)].
- [26] E. Nardi, J. Racker, and E. Roulet, *CP violation in scatterings, three body processes and the Boltzmann equations for leptogenesis*, *JHEP* **0709** (2007) 090, [[arXiv:0707.0378](#)].
- [27] S. Davidson, E. Nardi, and Y. Nir, *Leptogenesis*, *Phys. Rept.* **466** (2008) 105–177, [[arXiv:0802.2962](#)].
- [28] C. S. Fong, M. Gonzalez-Garcia, and J. Racker, *CP Violation from Scatterings with Gauge Bosons in Leptogenesis*, *Phys. Lett.* **B 697** (2011) 463–470, [[arXiv:1010.2209](#)].
- [29] C. Cheung and K. Ishiwata, *Baryogenesis with Higher Dimension Operators*, *Phys. Rev.* **D 88** (2013), no. 1 017901, [[arXiv:1304.0468](#)].
- [30] E. W. Kolb and M. S. Turner, *The Early Universe*. Westview Press, 1990.
- [31] D. Toussaint, S. B. Treiman, F. Wilczek, and A. Zee, *Matter - Antimatter Accounting, Thermodynamics, and Black Hole Radiation*, *Phys. Rev.* **D 19** (1979) 1036–1045.
- [32] A. Dolgov, *Baryon asymmetry of the universe and violation of the thermodynamic equilibrium.*, *Pisma Zh. Eksp. Teor. Fiz.* **29** (1979) 254–258.
- [33] S. M. Barr, *Comments on unitarity and the possible origins of the baryon asymmetry of the universe*, *Phys. Rev.* **D 19** (Jun, 1979) 3803–3807.
- [34] M. E. Peskin and D. V. Schroeder, *An Introduction to quantum field theory*. Addison-Wesley, 1995.
- [35] J. Edsjo and P. Gondolo, *Neutralino relic density including coannihilations*, *Phys. Rev.* **D 56** (1997) 1879–1894, [[hep-ph/9704361](#)].
- [36] W. Buchmuller and M. Plumacher, *Neutrino masses and the baryon asymmetry*, *Int. J. Mod. Phys.* **A 15** (2000) 5047–5086, [[hep-ph/0007176](#)].
- [37] Wolfram Research, Inc., *Mathematica Edition: Version 8.0*. 2010.
- [38] R. J. Scherrer and M. S. Turner, *Decaying particles do not “heat up” the universe*, *Phys. Rev. D* **31** (Feb, 1985) 681–688.
- [39] S. Hannestad, *Nonequilibrium effects on particle freezeout in the early universe*, *New Astron.* **4** (1999) 207–214, [[astro-ph/9903034](#)].

- [40] G. Giudice, A. Notari, M. Raidal, A. Riotto, and A. Strumia, *Towards a complete theory of thermal leptogenesis in the SM and MSSM*, *Nucl. Phys. B* **685** (2004) 89–149, [[hep-ph/0310123](#)].
- [41] A. Basboll and S. Hannestad, *Decay of heavy Majorana neutrinos using the full Boltzmann equation including its implications for leptogenesis*, *JCAP* **0701** (2007) 003, [[hep-ph/0609025](#)].
- [42] J. Garayoa, S. Pastor, T. Pinto, N. Rius, and O. Vives, *On the full Boltzmann equations for Leptogenesis*, *JCAP* **0909** (2009) 035, [[arXiv:0905.4834](#)].
- [43] F. Hahn-Woernle, M. Plumacher, and Y. Y. Y. Wong, *Full Boltzmann equations for leptogenesis including scattering*, *JCAP* **0908** (2009) 028, [[arXiv:0907.0205](#)].
- [44] M. Kawasaki, K. Kohri, and T. Moroi, *Hadronic decay of late - decaying particles and Big-Bang Nucleosynthesis*, *Phys. Lett. B* **625** (2005) 7–12, [[astro-ph/0402490](#)].
- [45] M. Kawasaki, K. Kohri, and T. Moroi, *Big-Bang nucleosynthesis and hadronic decay of long-lived massive particles*, *Phys. Rev. D* **71** (2005) 083502, [[astro-ph/0408426](#)].
- [46] K. Jedamzik, *Big bang nucleosynthesis constraints on hadronically and electromagnetically decaying relic neutral particles*, *Phys. Rev. D* **74** (2006) 103509, [[hep-ph/0604251](#)].
- [47] **Super-Kamiokande** Collaboration, K. Abe et al., *The Search for $n - \bar{n}$ oscillation in Super-Kamiokande I*, [arXiv:1109.4227](#).
- [48] M. Baldo-Ceolin et al., *A new experimental limit on neutron-antineutron oscillations*, *Zeitschrift für Physik C* **63** (1994) 409–416.
- [49] **Particle Data Group** Collaboration, J. Beringer et al., *Review of Particle Physics (RPP)*, *Phys. Rev. D* **86** (2012) 010001.
- [50] **BaBar** Collaboration, B. Aubert et al., *Observation of $B^+ \rightarrow \bar{K}^0 K^+$ and $B^0 \rightarrow K^0 \bar{K}^0$* , *Phys. Rev. Lett.* **97** (2006) 171805, [[hep-ex/0608036](#)].
- [51] Y.-T. Duh, T.-Y. Wu, P. Chang, G. Mohanty, Y. Unno, et al., *Measurements of Branching Fractions and Direct CP Asymmetries for $B \rightarrow K\pi$, $B \rightarrow \pi\pi$ and $B \rightarrow KK$ Decays*, *Phys. Rev. D* **87** (2013) 031103, [[arXiv:1210.1348](#)].
- [52] **Super-Kamiokande** Collaboration, K. Kobayashi et al., *Search for nucleon decay via modes favored by supersymmetric grand unification models in Super-Kamiokande-I*, *Phys. Rev. D* **72** (2005) 052007, [[hep-ex/0502026](#)].
- [53] D. Binosi and L. Theussl, *JaxoDraw: A Graphical user interface for drawing Feynman diagrams*, *Comput. Phys. Commun.* **161** (2004) 76–86, [[hep-ph/0309015](#)].